Original Article

Promotion of non-small cell lung cancer tumor growth by *FHL2* via inducing angiogenesis and vascular permeability

Tengfei Chen[1#], Jun Chen[2#], Qiuyun Chen[3], Zhipan Liang[1], Liuying Pan[1], Jun Zhao[2], Xiaowei She[1]

[1]Department of Thoracic Surgery, The Affiliated Suzhou Hospital of Nanjing Medical University, Suzhou Municipal Hospital, Gusu School, Nanjing Medical University, Suzhou, China; [2]Department of Thoracic Surgery, The First Affiliated Hospital of Soochow University, Medical College of Soochow University, Suzhou, China; [3]Department of Clinical Nursing, Dushu Lake Hospital Affiliated to Soochow University, Suzhou, China

Contributions: (I) Conception and design: J Zhao, X She; (II) Administrative support: X She; (III) Provision of study materials or patients: T Chen, J Chen, Z Liang, L Pan; (IV) Collection and assembly of data: T Chen, J Chen; (V) Data analysis and interpretation: T Chen, Q Chen; (VI) Manuscript writing: All authors; (VII) Final approval of manuscript: All authors.

[#]These authors contributed equally to this work.

Correspondence to: Xiaowei She, MD. Department of Thoracic Surgery, The Affiliated Suzhou Hospital of Nanjing Medical University, Suzhou Municipal Hospital, Gusu School, Nanjing Medical University, No. 458 Shizi Street, Gusu District, Suzhou 215031, China. Email: drshxw@163.com; Professor Jun Zhao, MD, PhD. Department of Thoracic Surgery, The First Affiliated Hospital of Soochow University, Medical College of Soochow University, No. 899 Pinghai Rd., Gusu District, Suzhou 215006, China. Email: junzhao@suda.edu.cn.

Background: Antiangiogenetic therapy is one of the effective strategies for non-small cell lung cancer (NSCLC) treatment. Four-and-a-half LIM-domain protein 2 (*FHL2*) serves as a key function in cell growth and metastasis of multiple cancers, but the role of *FHL2* in NSCLC angiogenesis has not been intensely examined.

Methods: *FHL2* expression in NSCLC tissues and cell lines and its correlation with patients prognosis were investigated by using The Cancer Genome Atlas (TCGA) database and quantitative polymerase chain reaction (qPCR). Cell Counting Kit-8 (CCK-8) assay, EdU (5-ethynyl-2'-deoxyuridine) assay, and a xenograft model were used to investigate the effects of *FHL2* on NSCLC progression *in vitro* and *in vivo*. CCK-8, wound-healing, Transwell invasion, tube formation, and permeability assays were performed to determine the roles of *FHL2* in angiogenesis and vascular permeability. Vascular endothelial growth factor A (VEGFA) enzyme-linked immunosorbent assay (ELISA) assay, Western blot analysis, and MK-2206 were used to investigate the specific mechanism mediated by *FHL2*.

Results: We demonstrated that *FHL2* was significantly upregulated in NSCLC tissues and cell lines and was associated with poor prognosis. *FHL2* overexpression enhanced the cell viability of NSCLC cells, as well as the proliferation, migration, invasion, and tube formation of human umbilical vein endothelial cells (HUVECs). In addition, we determined that *FHL2* activated the AKT-mTOR signaling pathway in HUVECs by promoting VEGFA secretion from NSCLC cells, thereby inducing angiogenesis and vascular leakiness. We further confirmed that *FHL2* also promoted NSCLC tumor growth *in vivo*.

Conclusions: Our study revealed the role of *FHL2* in NSCLC and the mechanism by which *FHL2* promotes NSCLC tumorigenesis, providing novel insights into targeted therapy for NSCLC.

Keywords: Non-small cell lung cancer (NSCLC); four-and-a-half LIM-domain protein 2 (*FHL2*); angiogenesis; permeability

Submitted Dec 29, 2023. Accepted for publication Feb 04, 2024. Published online Feb 23, 2024.
doi: 10.21037/jtd-23-1975
View this article at: https://dx.doi.org/10.21037/jtd-23-1975

Introduction

Lung cancer is the leading cause of cancer-related death worldwide, with increasing incidence and mortality (1), and non-small cell lung cancer (NSCLC) has been reported to account for over 80% of all lung cancers. It can be classified into three types, including lung squamous cell carcinoma (LUSC), lung adenocarcinoma (LUAD), and large-cell carcinoma, among which LUSC and LUAD are the most common subtypes (1). Due to the lack of early diagnosis, most patients with NSCLC are diagnosed with terminal-stage disease, with a 5-year survival rate of less than 15% (2).

Angiogenesis is one of the most critical steps in the development of NSCLC. It enables tumor growth and metastasis by providing cancer cells with nutrients and oxygen (3). During the growth of solid tumors, angiogenesis enables cancer cells to metastasize because newly formed blood vessels are leaky (4). Increased angiogenesis is correlated with the poor prognosis of patients with NSCLC (5). Recently, accumulating evidence has indicated that multiple cancer-associated genes drive NSCLC angiogenesis and vascular permeability by activating endothelial cells (6). For instance, *GOLPH3* promotes proliferation and angiogenesis of LUAD by regulating the Wnt/β-catenin signaling pathway (7).

The TRPV3 protein promotes NSCLC angiogenesis by activating hypoxia-inducible factor 1α (HIF-1α)-vascular endothelial growth factor (VEGF) signaling pathway (8). A disintegrin and metalloproteinase 17 (ADAM-17) inhibitor ZLDI-8 inhibits NSCLC angiogenesis by suppressing Notch1-HIF1α-VEGF signaling pathway (9). However, the molecular mechanism underlying the regulation of NSCLC angiogenesis and permeability has not been fully elucidated.

Four-and-a-half LIM-domain protein 2 (*FHL2*) can directly interact with several proteins and is involved in various biological progress including cell adhesion, proliferation, apoptosis, invasion, and differentiation (10). It is reported that *FHL2* can promote the progression of several cancers, such as ovarian cancer (11), cervical cancer (12), esophageal squamous-cell carcinoma (13), and NSCLC progression (14). A recent study showed that *FHL2* upregulation facilitated the proliferation and migration of NSCLC cells and exacerbated the negative outcomes of patients with NSCLC (14). More importantly, *FHL2* was identified as a biomarker and an invasion-promoting gene of LUAD progression (14,15). However, the role of *FHL2* in NSCLC angiogenesis and vascular permeability has not been elucidated. Therefore, it is critical to elucidate the specific mechanisms underlying the development of NSCLC.

In this study, *FHL2* was found to be highly expressed in NSCLC tissues and cell lines, capable of promoting cell proliferation, angiogenesis, and vascular permeability. Mechanistically, we demonstrated that *FHL2* regulated angiogenesis and vascular permeability in NSCLC cells by activating the VEGFR2-AKT-mTOR signaling pathway, indicating that this pathway can be a potential therapeutic target of NSCLC treatment. We present this article in accordance with the ARRIVE and MDAR reporting checklists (available at https://jtd.amegroups.com/article/view/10.21037/jtd-23-1975/rc).

Highlight box

Key findings

- This study revealed that four-and-a-half LIM-domain protein 2 (*FHL2*) promoted non-small cell lung cancer (NSCLC) angiogenesis and vascular permeability by enhancing the secretion of vascular endothelial growth factor A from NSCLC cells and activating the VEGFR2-AKT-mTOR signaling pathway in Human Umbilical Vein Endothelial Cells (HUVECs).

What is known and what is new?

- *FHL2* was identified as a biomarker of lung adenocarcinoma (LUAD), but precise mechanisms of *FHL2* in NSCLC angiogenesis are not fully understood.
- This study provided the first insights into the role and specific mechanism of *FHL2* in NSCLC angiogenesis and vascular permeability.

What is the implication, and what should change now?

- These findings indicating the VEGFR2-AKT-mTOR signaling pathway can be a potential therapeutic target of NSCLC treatment.
- Other potential mechanisms of *FHL2* in angiogenesis and vascular permeability remain to be investigated.

Methods

Data collection

Using The Cancer Genome Atlas (TCGA) database, we gathered FPKM RNA-seq data from LUAD cases and LUSC cases. Based on these TCGA database, we applied the ggplot2 package to visualize the differential expression of *FHL2* mRNA in TCGA normal tissues and TCGA cancer tissues. The survival curves were plotted using ggplot2 packages. The study was conducted in accordance with the Declaration of Helsinki (as revised in 2013).

Regents and antibodies

MK-2206 (#HY-108232) was purchased from MedChemExpress (Monmouth Junction, NJ, USA). β-actin (#3700), Flag (#14793S), p-AKT (#4060), t-AKT (#4691), p-mTOR (#5536), and t-mTOR (#2983) antibodies were purchased from Cell Signaling Technology (Danvers, MA, USA); FHL2 (#ab202584) and VEGFA (#ab1316) antibodies from Abcam (Cambridge, UK); and VEGFR2 (#66828-1-Ig) antibody from Proteintech Group, Inc. (Rosemont, IL, USA).

Cell culture

Human umbilical vein endothelial cells (HUVECs), normal human bronchial endothelial (HBE) cells, and NSCLC cell lines (A549, H460, H1299, H226, and H520) were purchased from the American Type Culture Collection (ATCC; Manassas, VI, USA). HUVECs were cultured in Dulbecco's Modified Eagle's Medium (DMEM)/F12 Medium (HyClone, Logan, UT, USA) supplemented with 10% fetal bovine serum (FBS; Gibco, Thermo Fisher Scientific, Waltham, MA, USA). The NSCLC and HBE cell lines were cultured in RPMI-1640 medium containing 10% FBS. All cells were cultured at 37 ℃ in a 5% CO_2 atmosphere.

Plasmid and small interfering RNA transfection

Flag-*FHL2* plasmids were synthesized by GENEWIZ (South Plainfield, NJ, USA). *FHL2* small interfering RNA (siRNA) and VEGFA siRNA were purchased from GenePharma (Shanghai, China). A549 and H226 cells were seeded into 6-well plates and transfected with siRNA or plasmids using Lipofectamine 2000 (Invitrogen, Thermo Fisher Scientific, Waltham, MA, USA) according to manufacturer's instructions.

Western blot analysis

Cells were lysed in RIPA lysis buffer (Beyotime, Haimen, China) for 30 min. Bicinchoninic acid (BCA) protein assay kit (Takara Bio, Kusatsu, Japan) was used to quantify protein concentration. Samples were separated with sodium dodecyl sulfate-polyacrylamide gel electrophoresis (SDS-PAGE) and then transferred to a polyvinylidene fluoride (PVDF) membrane (MilliporeSigma, Burlington, MA, USA). After 1-h blocking in 5% nonfat milk, membranes were incubated with primary antibody overnight at 4 ℃. Subsequently, membranes were washed with tris-buffered saline with Tween20 (TBST) for three times and then incubated with secondary antibody at room temperature for 1 h. Bands were visualized by using enhanced chemiluminescence (ECL) detection kit (MilliporeSigma) after three washes.

Real-time polymerase chain reaction analysis

Total RNA was isolated with TRIzol reagent (Invitrogen). RNA was then reverse- transcribed into complement DNA (cDNA) by using a PrimeScript™ RT Master Mix Kit (Takara Bio). Real-time polymerase chain reaction (RT-PCR) was performed by using cDNA and a SYBR Green qPCR Master Mix (Takara Bio) according to manufacturer's instructions. For each sample, experiments were performed in triplicate, and all results were normalized to β-actin expression. The primers for quantitative PCR (qPCR) are listed in Table S1.

Conditioned medium (CM) preparation

A549 and H226 cells transfected with plasmids or siRNA were cultured under RPMI-1640 medium containing 10% FBS for 48 h. The supernatant was then collected, centrifuged, and filtered through a 0.22-μm filter (MilliporeSigma).

Cell viability assay

In brief, 5.0×10^3 cells were seeded into 96-well plates, and Cell Counting Kit-8 (CCK-8; Dojindo, Kumamoto, Japan) was used to detect cell viability according to the manufacturer's instructions.

EdU assay

An EdU (5-ethynyl-2'-deoxyuridine) assay kit (Beyotime) was used to evaluate cell proliferation according to manufacturer's instructions. Briefly, A549 and H226 cells were transfected with plasmids or siRNA and then incubated with EdU for 2 h, which was followed by the staining of nuclei with DAPI (4',6-diamidino-2-phenylindole). Cells were fixed with 4% paraformaldehyde for 15 min at room temperature. Subsequently, EdU-positive cells were analyzed with a fluorescence microscope (Olympus, Tokyo, Japan).

Wound-healing assay

HUVECs were seeded into 6-well plates in confluent monolayers. Scratch wounds were created by using a sterilized tip in CM. Images were captured at 0 and 24 h after a wash three times with phosphate-buffered saline (PBS).

Cell invasion assay

HUVECs (2.5×10^5) in CM were seeded in the top chamber of Transwell inserts (0.4 μm; Corning, Corning, NY, USA) coated with Matrigel, and 600 μL of medium containing 20% FBS were added to the lower chambers. After 24 h, cells on the upper chamber were removed, and cells on the lower surfaces were fixed with 0.1% crystal violet and photographed.

Tube formation assay

For tube formation assay, 96-well plates were coated with 50 μL of Matrigel at 37 ℃ for 1 h. HUVECs (2.0×10^5) in CM with or without MK-2206 were seeded into the Matrigel precoated 96-well plates. After 12 h, tubes were imaged and counted under an inverted microscope.

VEGFA enzyme-linked immunosorbent assay (ELISA)

VEGFA levels in CM were detected using an ELISA kit (Abcam) according to the manufacturer's instructions. Optical density (OD) values were measured with a plate reader.

Endothelial permeability analysis

HUVECs (1.0×10^5) in CM were seeded in the top chamber of Transwell inserts (0.8 μm; Corning) for 72 h. Rhodamine B isothiocyanate-dextran (0.1 mg/mL; average mol wt ~70,000; MilliporeSigma) was added to the top well, and PBS was added to the bottom well. After 30 min, the medium in the lower chamber was collected, and the fluorescence intensity was analyzed at 544-nm excitation and 590-nm emission.

Tumor xenografts

Experiments were performed under a project license (No. 202105A436) granted by ethics board of Soochow University, in compliance with institutional guidelines for the care and use of animals. A protocol was prepared before the study without registration. Six-week-old nude mice were purchased from Shanghai Laboratory Animal Center (Shanghai, China). A549 cells transfected with lentivirus vector 10 (LV10) or LV10-sh*FHL2* (5.0×10^7/mL) were collected and mixed with Matrigel (Corning) at a 1:1 ratio v/v. Following this, 100 μL of cells were injected subcutaneously into the back region of nude mice. Each group contained five mice. Tumor size and mice body weight were measured every other day, and the volume was calculated according to the following formula:

$$Volume = \frac{a \times b^2}{2} \quad [1]$$

where a = length, b = width.

Statistical analysis

All statistical analyses were performed with GraphPad Prism software (GraphPad Software, Inc., San Diego, CA, USA). Comparisons among groups were performed using one-way analysis of variance (ANOVA) or Student *t*-test. All data are presented as the mean ± standard deviation (SD). A P value <0.05 was considered statistically significant.

Results

FHL2 was highly expressed in NSCLC tissues and correlated with poor prognosis

To provide initial insight into the clinical relevance of *FHL2* expression in NSCLC tissues, the messenger RNA (mRNA) level of *FHL2* was analyzed from TCGA database. *FHL2* was found to be highly expressed among patients with LUAD and LUSC at stages I, II, III, and IV compared to normal tissue (*Figure 1A-1C*). Patients with stage III LUAD showed increased *FHL2* expression compared to patients at stage I (*Figure 1B*). Patients with LUSC with distant metastasis (stage IV) presented the highest *FHL2* expression when compared to patients at stages I, II, and III, but with no statistical significance (*Figure 1C*). Furthermore, high levels of *FHL2* expression predicted poor prognosis in patients with NSCLC (*Figure 1D,1E*).

We also evaluated *FHL2* expression level in NSCLC cell lines by using qPCR analysis. We found that *FHL2* expression was obviously increased in LUAD cell lines (A549, H460, and H1299) and LUSC cell lines (H226 and H520) (*Figure 1F*). A549 and H226 cells were selected to be used in later experiments.

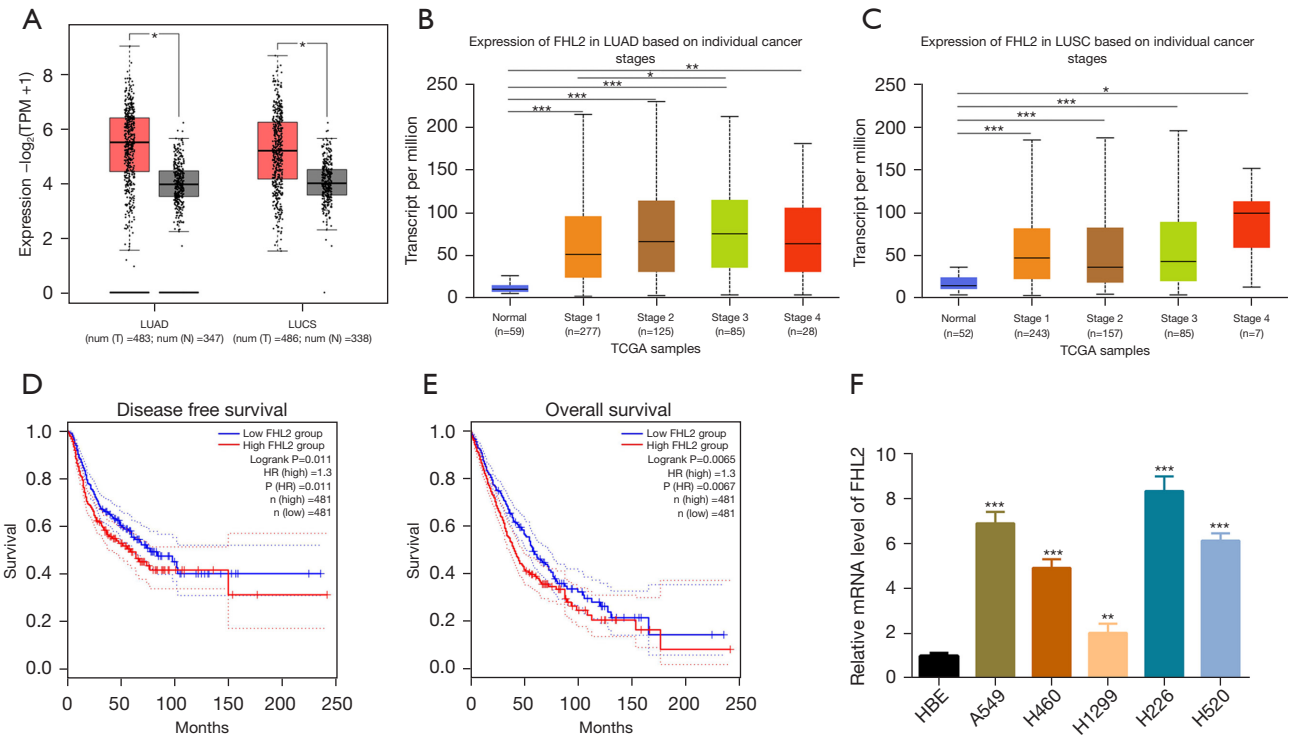

Figure 1 *FHL2* expression in NSCLC tissues and cell lines. (A) *FHL2* mRNA expression in LUAD and LUSC tissues from TCGA database. (B,C) *FHL2* expression in LUAD (B) and LUSC (C) tissues at different stages from TCGA database. (D,E) Disease-free survival (D) and overall survival (E) of patients with NSCLC with low or high levels of *FHL2*. (F) *FHL2* mRNA expression in NSCLC cell lines was detected via qPCR. *, P<0.05; **, P<0.01; ***, P<0.001. TPM, transcript per million; LUAD, lung adenocarcinoma; LUSC, lung squamous cell carcinoma; TCGA, The Cancer Genome Atlas; HR, hazard ratio; *FHL2*, four-and-a-half LIM-domain protein 2; NSCLC, non-small cell lung cancer; mRNA, messenger RNA; qPCR, quantitative polymerase chain reaction.

FHL2 promoted NSCLC cell proliferation in vitro

To further explore the role of *FHL2* in NSCLC cell proliferation, we investigated the viability of A549 and H226 cells after overexpression of *FHL2* or disruption of its transcript via siRNA targeting. The FHL2 expression was detected by using qPCR and Western blot analysis (Figure S1A,S1B and *Figure 2A,2B*), and CCK-8 assays were performed to detect cell viability. We observed that proliferation was enhanced by *FHL2* overexpression and weakened by *FHL2* silencing (*Figure 2C,2D*). Similar results were also validated by EdU assays, in which *FHL2* overexpression increased the EdU-incorporated cell proportion and *FHL2* silencing reduced the EdU-incorporated cell proportion (*Figure 2E,2F*), suggesting that *FHL2* could promote NSCLC cell proliferation.

FHL2 promoted angiogenesis and vascular permeability in vitro

The proliferation, migration, and invasion of HUVECs are key steps in tumor angiogenesis (16), and we thus explored the effects of *FHL2* on these features. To evaluate the functional significance of *FHL2* in tumor angiogenesis, we collected the CM from *FHL2*-overexpressed or -silenced A549 and H226 cells and used as it as the culture media for HUVECs. CM derived from *FHL2*-overexpressed A549 and H226 cells significantly promoted proliferation (*Figure 3A*) and markedly increased the migration and invasion capacities of HUVECs (*Figure 3B,3C*). On the other hand, CM derived from *FHL2*-silenced A549 and H226 inhibited the proliferation (*Figure 3D*), migration, and invasion (*Figure 3E,3F*) of HUVECs. We further investigated

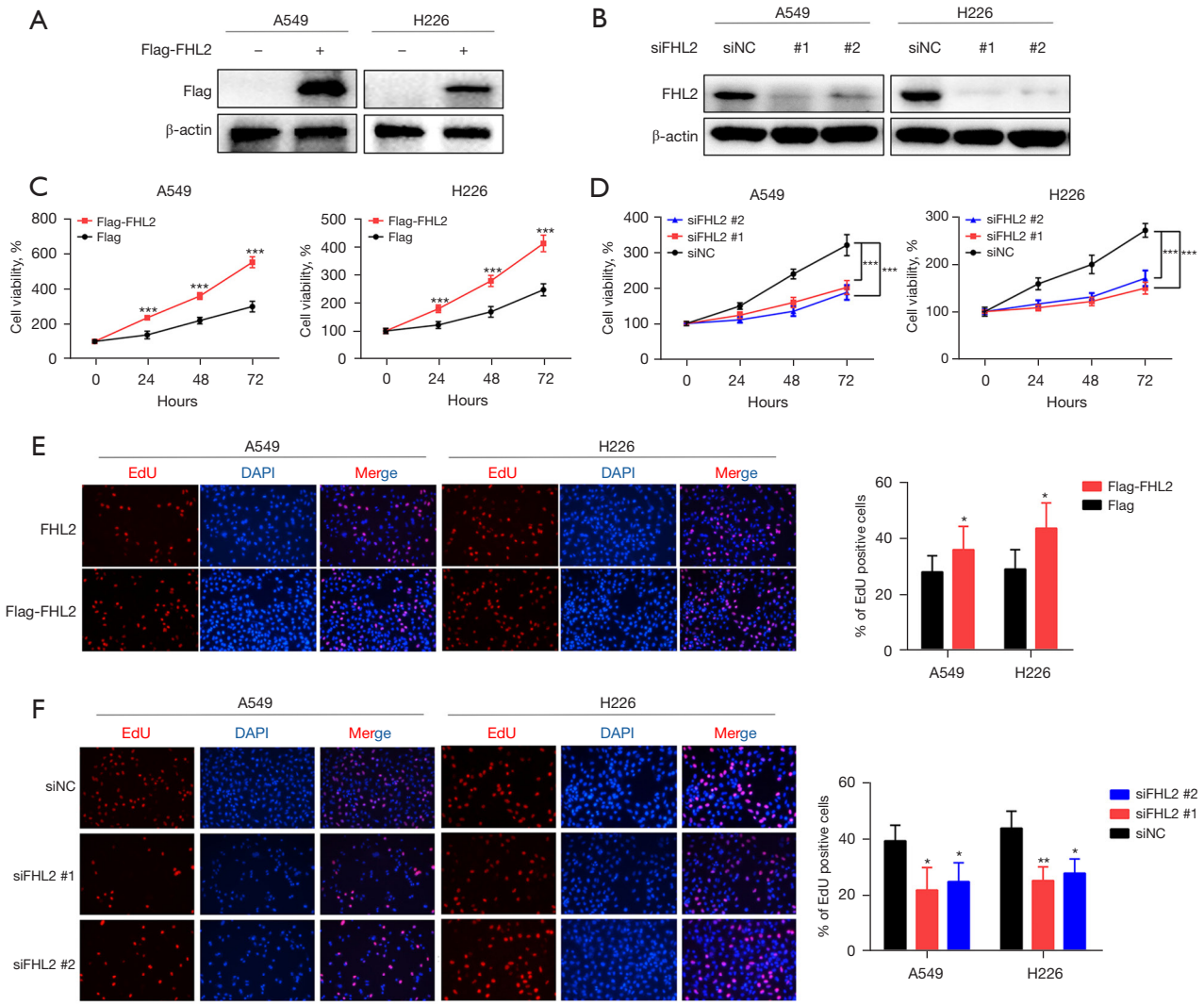

Figure 2 *FHL2* promoted proliferation of NSCLC cells *in vitro*. (A) *FHL2* protein expression upon transfection with Flag-FHL2 plasmids. (B) *FHL2* protein expression upon transfection with siRNA targeting *FHL2*. (C) CCK-8 assay for investigating *FHL2* overexpression effects on the proliferation of A549 and H226 cells. (D) CCK-8 assay for investigating *FHL2* silencing effects on the proliferation of A549 and H226 cells. (E) EdU assay for evaluation of *FHL2* overexpression effects on the proliferation of A549 and H226 cells (magnification ×100). (F) EdU assay for evaluation of *FHL2* overexpression effects on the proliferation of A549 and H226 cells (magnification ×100). The independent assays were replicated three times. Mean "±" SD are provided. *, P<0.05; **, P<0.01; ***, P<0.001. *FHL2*, four-and-a-half LIM-domain protein 2; NSCLC, non-small cell lung cancer; CCK-8, Cell Counting Kit-8; SD, standard deviation.

the effects of *FHL2* on HUVEC tube formation ability, which involves all steps of angiogenesis (17). The results demonstrated that the number of complete meshes induced by CM derived from *FHL2*-overexpressed cells was significantly increased (*Figure 3G*), while CM derived from *FHL2*-silenced cells led to a reduced number of complete meshes, suggesting that *FHL2* could promote NSCLC angiogenesis (*Figure 3H*). To further explore the roles of *FHL2* in NSCLC angiogenesis, we analyzed the correlation between *FHL2* and *CD146*, an endothelial cell marker (18), in tissue samples from TCGA database. *FHL2* expression was found to be positively associated with *CD146* expression in NSCLC tissues (Figure S1C).

Active angiogenesis and increased vascular permeability are critical factors that facilitate tumor growth (19). In this study, we assessed the effects of *FHL2* on the permeability of

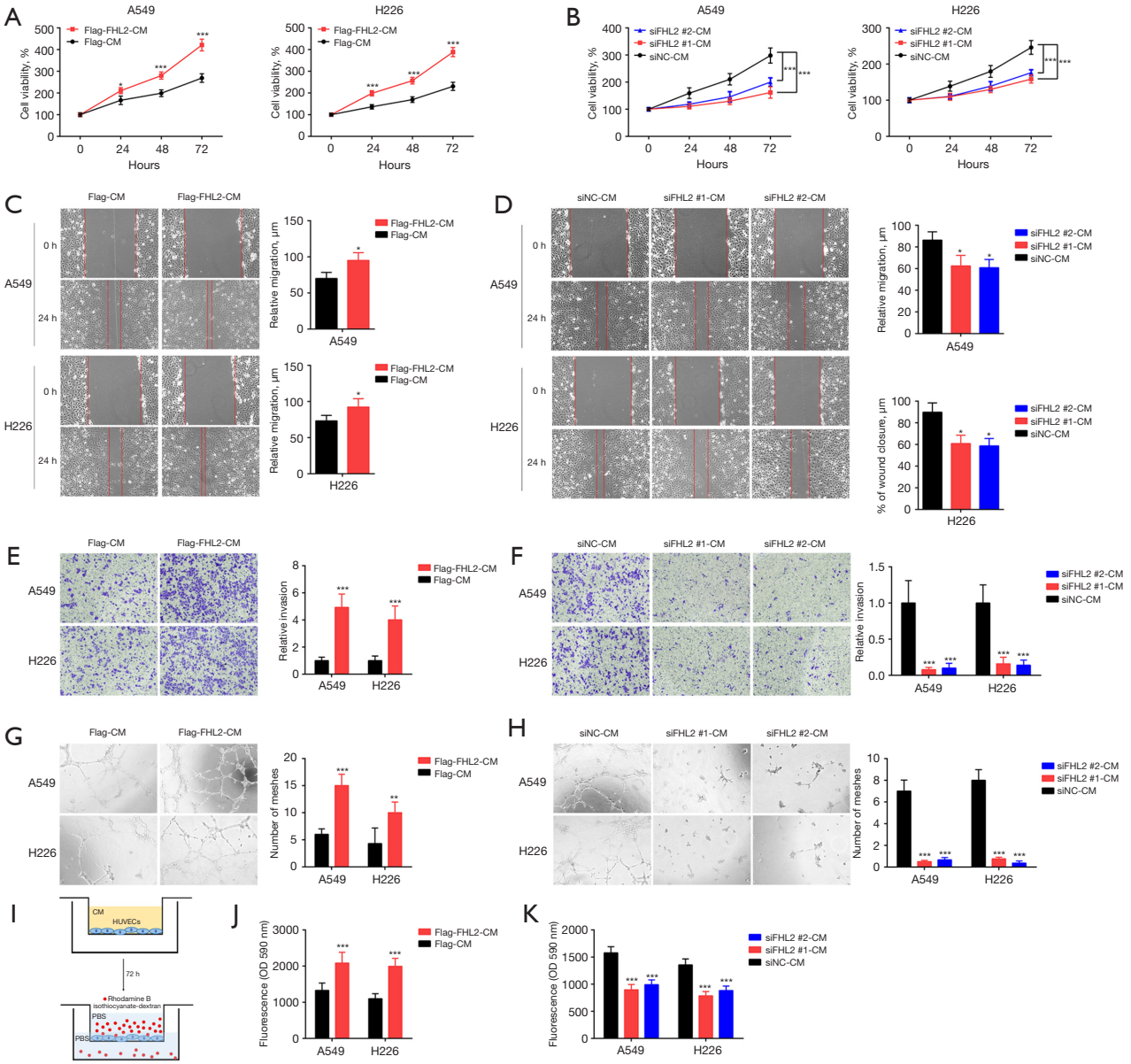

Figure 3 *FHL2* promoted the proliferation, migration, invasion, and tube formation of HUVECs *in vitro*. (A,B) CCK-8 assays for investigating the effects of CM from *FHL2*-overexpressed (A) or *FHL2*-silenced (B) NSCLC cells on the proliferation of HUVECs. (C,D) Wound-healing assays evaluating migration effects of CM from *FHL2*-overexpressed (magnification ×100) (C) or *FHL2*-silenced (D) NSCLC cells on HUVECs. (E,F) Transwell invasion assays for investigation of invasion effects of CM from *FHL2*-overexpressed (E) or *FHL2*-silenced (F) NSCLC cells on HUVECs. Crystal-violet-stained HUVECs (magnification ×100). (G,H) The effects of CM from *FHL2*-overexpressed (G) or *FHL2*-silenced (H) NSCLC cells on tube formation in HUVECs. Capillary tube structure was photographed under a ×100 bright-field microscope. The number of meshes are shown in the bar graph. (I) HUVECs in CM were grown on the inserts of a dual-well plate for 72 h to form the endothelial monolayer. Rhodamine B isothiocyanate-dextran (70 kDa) was added into the upper chamber. The fluorescence in the bottom chamber was measured. (J,K) Permeability of the HUVECs monolayers to Rhodamine B isothiocyanate-dextran after exposure to the CM from *FHL2*-overexpressed (J) or *FHL2*-silenced (K) NSCLC cells for 72 h. The independent assays were replicated three times. Mean "±" SD are provided. *, P<0.05; **, P<0.01; ***, P<0.001. *FHL2*, four-and-a-half LIM-domain protein 2; HUVEC, human umbilical vein endothelial cell; CCK-8, Cell Counting Kit-8; NSCLC, non-small cell lung cancer; CM, conditioned medium; SD, standard deviation; OD, optical density; PBS, phosphate-buffered saline.

the endothelial monolayer. The changes in the permeability of endothelial monolayer after the treatment of CM derived from A549 and H226 cells were detected by measuring the traversing of rhodamine-labeled dextran through HUVEC monolayers. Treatment with the CM derived from *FHL2*-overexpressed cells significantly increased the passing of dextran through the HUVEC monolayer (*Figure 3I,3J*), while the traverse of dextran was reduced in the CM derived from *FHL2*-silenced cells (*Figure 3K*). These results suggest that *FHL2* could increase vascular permeability *in vitro*.

FHL2 promoted angiogenesis through VEGFR2-AKT-mTOR signaling pathway

There are many pathways involved in tumor angiogenesis, among which *VEGFA* is reported to play a critical role (20). Consequently, we examined the mRNA expression of several angiogenesis-related cytokines in A549 cells after *FHL2* silencing and found that the mRNA expression of *VEGFA* was significantly downregulated (*Figure 4A*). This finding was corroborated by ELISA results, in which the VEGFA concentration was reduced (*Figure 4B*). Moreover, the ELISA assay demonstrated that *FHL2* overexpression increased the level of VEGFA in NSCLC cells (*Figure 4C*). In addition, VEGFR2 is the main receptor for VEGF on endothelial cells, and it is involved in regulation of its downstream effectors, including AKT-mTOR signaling (21,22). Hence, we hypothesized that *FHL2* promotes NSCLC angiogenesis by inducing VEGFA secretion and then activating VEGFR2-AKT-mTOR signaling. Increased VEGFR2, p-AKT, and p-mTOR expression were observed in HUVECs after treatment with CM derived from *FHL2*-overexpressed NSCLC cells, and the AKT inhibitor MK-2206 reduced p-AKT and p-mTOR expression (*Figure 4D,4E*). Furthermore, attenuated HUVEC proliferation, migration, invasion, and angiogenesis were observed after incubation with MK-2206 (*Figure 4F-4I*), suggesting that the VEGFR2-AKT-mTOR signaling pathway participates in FHL2-induced NSCLC angiogenesis.

FHL2 increased vascular permeability through VEGFR2-AKT-mTOR signaling pathway

VEGFA regulates vascular permeability by activating VEGFR2, which is followed by the activation of AKT-mTOR signaling (21,23). Thus, we examined whether VEGFR2-AKT-mTOR signaling pathway is involved in *FHL2*-induced vascular leakiness. Two siRNAs targeting *VEGFA* were used to knockdown the expression of VEGFA in NSCLC cells (*Figure 5A,5B*). We found that VEGFA silencing significantly decreased *FHL2*-overexpressed induced vascular leakiness (*Figure 5C*). To further investigate the function of AKT-mTOR signaling in vascular permeability, HUVECs were co-cultured with MK-2206 and CM derived from *FHL2*-overexpressed NSCLC cells. As shown in *Figure 5D*, the effect of CM to enhance the transport of dextran was abrogated by MK-2206. Taken together, these findings suggest that *FHL2* could increase NSCLC vascular permeability through activation of the VEGFR2-AKT-mTOR signaling pathway.

FHL2 promoted NSCLC tumor growth in vivo

To further demonstrate the effect of *FHL2* on NSCLC tumor growth *in vivo*, mice were subcutaneously injected with A549-*shFHL2* cells (*Figure 6A*). We then monitored tumor volumes and mice body weight every other day. We found that the stable knockdown of *FHL2* remarkably reduced the tumor volume and weights (*Figure 6B,6C*), while no significant difference in mice body weight was observed (*Figure 6D*). These results indicate that *FHL2* might facilitate NSCLC tumor growth *in vivo*.

Discussion

NSCLC is a malignant tumor that seriously threatens human life and has become a leading cause of cancer death in the world (1). The occurrence and development of NSCLC is regulated by a variety of cancer-related genes, and the underlying mechanisms of NSCLC progression have still yet to be clarified. It is known that tumor angiogenesis is a critical step in NSCLC progression, and inhibition of angiogenesis to attenuate tumor growth is an effective strategy for NSCLC therapy (24).

FHL2, a member of FHL family, has been reported to be associated with the development of many types of cancers (10,12,25), playing different roles as a tumor-suppressor gene or an oncogene in different cancer types. For instance, *FHL2* may suppress the growth and differentiation of colorectal cancer cells (26) but promote cervical cancer cell tumor progression through the regulation of AKT-mTOR pathway (27). Recently, *FHL2* was identified as a biomarker of LUAD that could promote NSCLC progression and

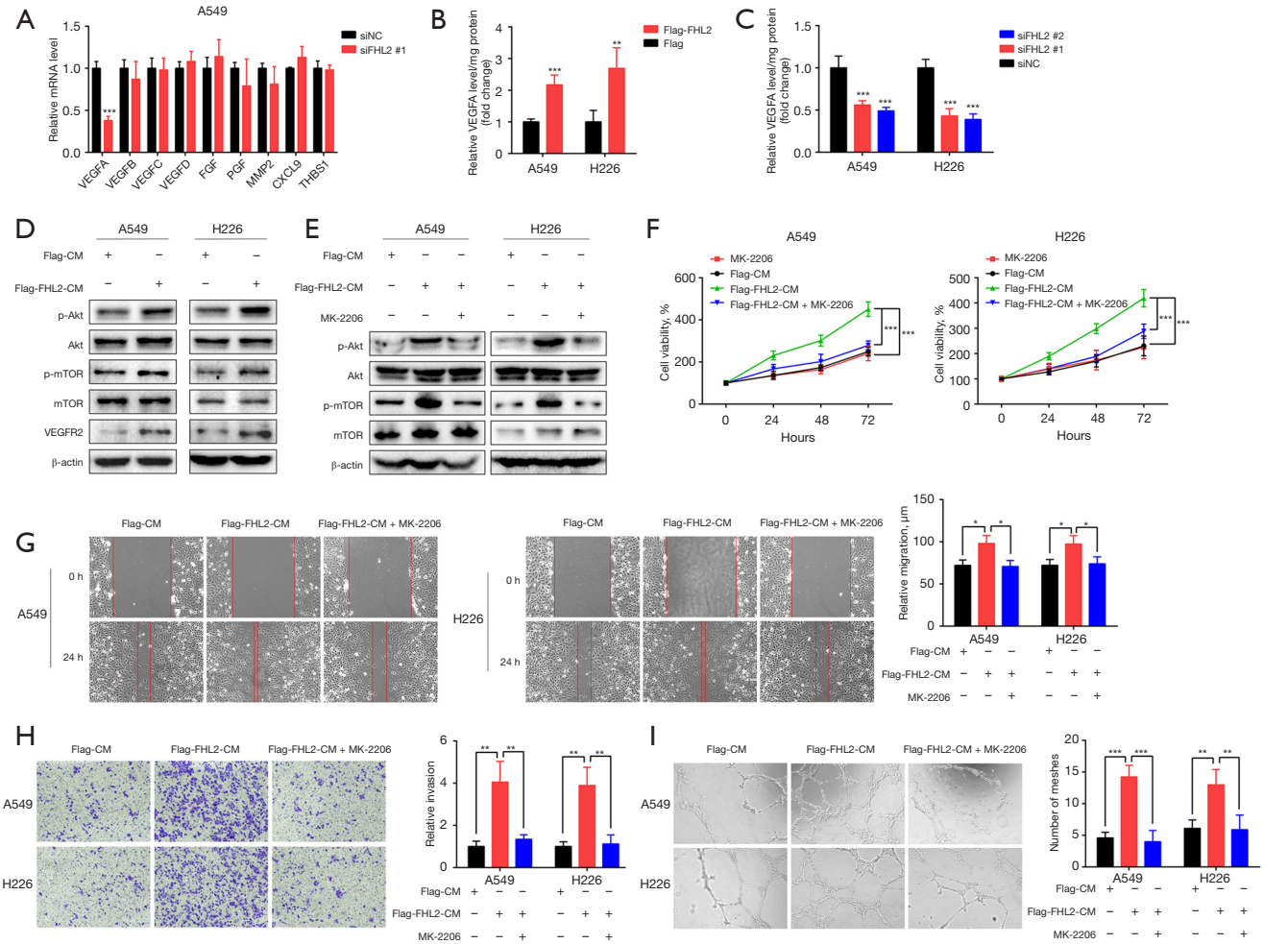

Figure 4 *FHL2* promoted NSCLC angiogenesis through the VEGFR2-AKT-mTOR signaling pathway. (A) The expression of angiogenesis-related genes was detected with qPCR in *FHL2*-silenced A549 cells. (B,C) The protein concentration of VEGFA in the CM from *FHL2*-overexpressed (B) or *FHL2*-silenced (C) NSCLC cells was analyzed via ELISA assays. (D) The expression of VEGFR2, p-AKT, and p-mTOR in HUVECs after the treatment with the CM from *FHL2*-silenced NSCLC cells for 72 h. (E) The expression of p-AKT and p-mTOR in HUVECs after co-culture with MK-2206 and the CM from *FHL2*-silenced NSCLC cells for 72 h. (F) Cell viability of HUVECs was examined by CCK-8 assay after co-culture with MK-2206 and the CM from FHL2-silenced NSCLC cells. (G) Migration ability of HUVECs was examined by wound-healing assay after co-culture with MK-2206 and the CM from *FHL2*-silenced NSCLC cells for 24 h (magnification ×100). (H) The invasion ability of HUVECs was examined by Transwell assay after co-culture with MK-2206 and the CM from *FHL2*-silenced NSCLC cells for 24 h. Crystal-violet-stained HUVECs (magnification ×100). (I) Tube formation ability of HUVECs was examined after co-culture with MK-2206 and the CM from *FHL2*-silenced NSCLC cells for 24 h. Capillary tube structure was photographed under a ×100 bright-field microscope. The number of meshes are shown in the bar graph. Data from three independent assays were pooled. Mean "±" SD are provided. *, P<0.05; **, P<0.01; ***, P<0.001. *FHL2*, four-and-a-half LIM-domain protein 2; NSCLC, non-small cell lung cancer; qPCR, quantitative polymerase chain reaction; VEGFA, vascular endothelial growth factor A; CM, conditioned medium; ELISA, enzyme-linked immunosorbent assay; HUVEC, human umbilical vein endothelial cell; CCK-8, Cell Counting Kit-8; SD, standard deviation.

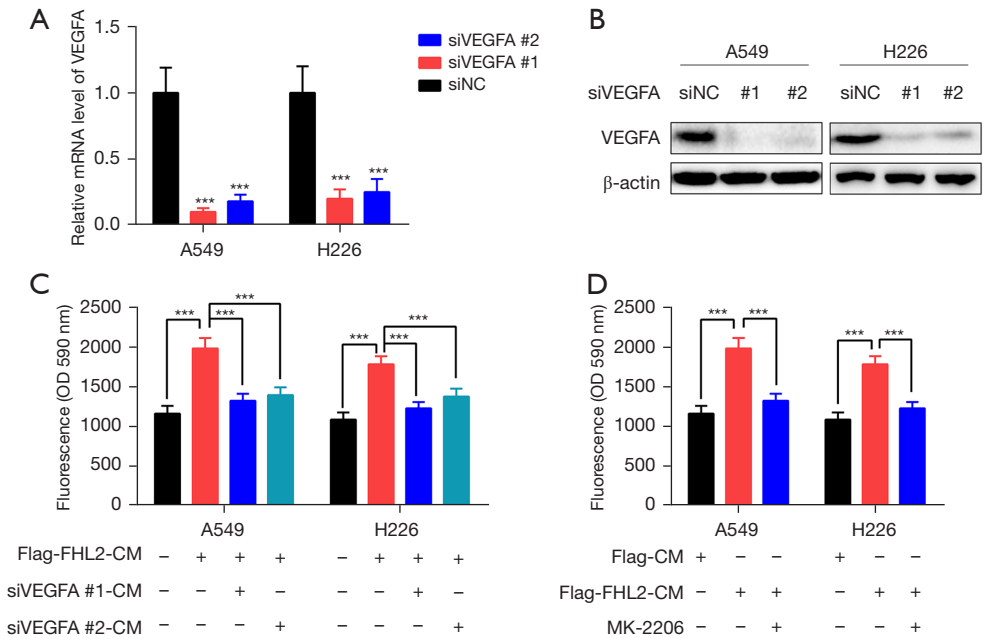

Figure 5 *FHL2* induced vascular permeability through the VEGFR2-AKT-mTOR signaling pathway. (A,B) The expression of VEGFA mRNA (A) and protein (B) upon transfection with siRNA targeting VEGFA in A549 and H226 cells. (C) Permeability of the HUVEC monolayers to Rhodamine B isothiocyanate-dextran after exposure to the CM from *FHL2*-overexpressed or VEGFA-silenced NSCLC cells. (D) Permeability of the HUVEC monolayers to Rhodamine B isothiocyanate-dextran after exposure to the CM from *FHL2*-overexpressed NSCLC cells and MK-2206. The independent assays were conducted three times. Mean "±" SD are provided. ***, P<0.001. OD, optical density; *FHL2*, four-and-a-half LIM-domain protein 2; VEGFA, vascular endothelial growth factor A; mRNA, messenger RNA; HUVEC, human umbilical vein endothelial cell; CM, conditioned medium; NSCLC, non-small cell lung cancer; SD, standard deviation.

migration (14). Our study reached similar conclusions. Specifically, *FHL2* was highly expressed in NSCLC tissues and cell lines, and this high level was correlated with the poor prognosis of patients with NSCLC. Moreover, *FHL2* overexpression was found to promote the proliferation of NSCLC cells, while *FHL2* silencing markedly inhibited NSCLC tumor growth *in vitro* and *in vivo*. Xenograft mice with *FHL2*-silenced NSCLC cells exhibited decreased tumor volume and weight. Despite these findings, the roles of *FHL2* in angiogenesis and vascular permeability, along with its underlying mechanism, still remain to be clarified by further investigation.

Angiogenesis is supported by dynamic endothelial cell functions, such as proliferation, migration, invasion, and tube formation, which are essential to the formation of vessel sprouts (6,28). In this study, we explored the roles of *FHL2* in NSCLC angiogenesis and vascular permeability, as well as its underlying mechanisms. We found that the CM from *FHL2*-overexpressed NSCLC cells significantly enhanced the abilities of HUVEC proliferation, migration, invasion, and tube formation *in vitro*, while CM from *FHL2*-silenced NSCLC cells markedly suppressed these features, suggesting that *FHL2* overexpression promotes NSCLC angiogenesis. In addition, increased vascular permeability is a characteristic of tumor vessels and results from excessive angiogenesis (5,29). *In vitro* permeability measurements revealed that the CM derived from *FHL2*-overexpressed NSCLC cells significantly enhanced vascular permeability, while the CM from *FHL2*-silenced cells prevented vascular leakage. Furthermore, a positive correlation between *FHL2* and *CD146* in NSCLC tissues was observed from TCGA database. Taken together, these results indicate that *FHL2* plays an essential role in the regulation of NSCLC angiogenesis and vascular permeability.

Angiogenesis is a complex process, tightly regulated by certain growth factors, receptors, and humoral factors (30). Among all the identified angiogenic pathways, the most critical one appears to be VEGFA/VEGFR signaling pathway, which is the main driver of vascular permeability via the activation of VEGFR2 (31). VEGFA binds to

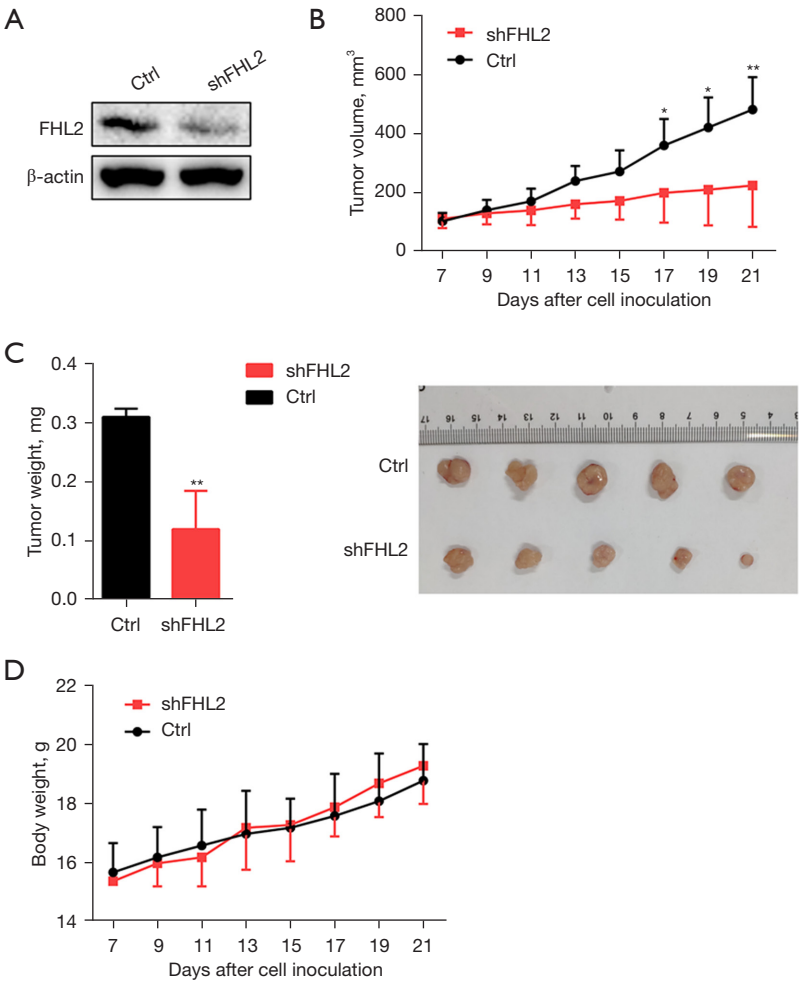

Figure 6 *FHL2* silencing inhibited NSCLC tumor growth *in vivo*. (A) The expression of *FHL2* protein in stable *FHL2*-silenced A549 cells (A549-sh*FHL2*). (B) Growth curve of A549-sh*FHL2* tumors in nude mice (n=5). (C) Tumor weight and photos of A549-sh*FHL2* tumors. (D) Body weight of tumor-bearing mice. Mean "±" SD are provided. *, P<0.05; **, P<0.01. *FHL2*, four-and-a-half LIM-domain protein 2; NSCLC, non-small cell lung cancer; SD, standard deviation.

VEGFR2 on the surface of endothelial cells to stimulate the AKT-mTOR downstream signaling pathway, thereby exerting its biological functions, such as angiogenesis and vascular permeability (20,32,33). *VEGFA* is upregulated in NSCLC tissues and has been associated with an increased risk of recurrence, metastasis, and death of patients with NSCLC (34). Hence, we further detected the VEGFA levels in the CM derived from NSCLC cells. VEGFA levels in the CM from *FHL2*-overexpressed NSCLC cells were significantly increased, while *FHL2* silencing reduced the protein levels. These findings indicate that *FHL2* can promote VEGFA secretion from NSCLC cells. Consistent with previous studies (20,23), we found that the CM derived from *FHL2*-overexpressed NSCLC cells increased the expression of VEGFR2, p-AKT, and p-mTOR in HUVECs by promoting VEGFA secretion. Moreover, *FHL2* induced the proliferation, migration, invasion, and tube formation of HUVECs, while vascular leakage was inhibited by MK-2206 and *VEGFA* silencing. Collectively, our results confirmed that *FHL2* significantly promoted tumor angiogenesis and vascular permeability by stimulating the VEGFR2-AKT-mTOR signaling pathway.

This study has been able to provide the first insights into the role and specific mechanism of *FHL2* in NSCLC angiogenesis and vascular permeability. In summary, we determined that *FHL2* is upregulated in NSCLC tissues

and cell lines and is associated with poor prognosis. Both *in vitro* and *in vivo*, *FHL2* was shown to exert a critical function in NSCLC progression by promoting NSCLC cell proliferation. In addition, *FHL2* promoted NSCLC angiogenesis and vascular permeability by enhancing the secretion of VEGFA from NSCLC cells and consequently activating the VEGFR2-AKT-mTOR signaling pathway in HUVECs (Figure S2). These findings point to *FHL2* as a potential therapeutic target for NSCLC treatment.

Conclusions

Our study demonstrated the role and specific mechanism of *FHL2* in NSCLC progression. Firstly, we found that *FHL2* was significantly upregulated in NSCLC tissues, which was associated with poor prognosis. In addition, *FHL2* could promote NSCLC cell proliferation. Furthermore, we determined that *FHL2* activated the VEGFR2-AKT-mTOR signaling pathway in HUVECs via promoting VEGFA secretion from NSCLC cells, thereby inducing angiogenesis. Our study revealed the role of *FHL2* in NSCLC and the mechanism by which *FHL2* promoted NSCLC tumorigenesis, providing a new sight on targeted therapy for NSCLC.

Acknowledgments

Funding: This work was supported by the National Natural Science Foundation of China (No. 81672934).

Footnote

Reporting Checklist: The authors have completed the ARRIVE and MDAR reporting checklists. Available at https://jtd.amegroups.com/article/view/10.21037/jtd-23-1975/rc

Data Sharing Statement: Available at https://jtd.amegroups.com/article/view/10.21037/jtd-23-1975/dss

Peer Review File: Available at https://jtd.amegroups.com/article/view/10.21037/jtd-23-1975/prf

Conflicts of Interest: All authors have completed the ICMJE uniform disclosure form (available at https://jtd.amegroups.com/article/view/10.21037/jtd-23-1975/coif). The authors have no conflicts of interest to declare.

Ethical Statement: The authors are accountable for all aspects of the work in ensuring that questions related to the accuracy or integrity of any part of the work are appropriately investigated and resolved. The study was conducted in accordance with the Declaration of Helsinki (as revised in 2013). Experiments were performed under a project license (No. 202105A436) granted by ethics board of Soochow University, in compliance with institutional guidelines for the care and use of animals.

References

1. Siegel RL, Miller KD, Fuchs HE, et al. Cancer Statistics, 2021. CA Cancer J Clin 2021;71:7-33.
2. Xie E, Lin M, Sun Z, et al. Serum miR-27a is a biomarker for the prognosis of non-small cell lung cancer patients receiving chemotherapy. Transl Cancer Res 2021;10:3458-69.
3. Hassan A, Badr M, Abdelhamid D, et al. Design, synthesis, in vitro antiproliferative evaluation and in silico studies of new VEGFR-2 inhibitors based on 4-piperazinylquinolin-2(1H)-one scaffold. Bioorg Chem 2022;120:105631.
4. Lu X, Friedrich LJ, Efferth T. Natural products targeting tumour angiogenesis. Br J Pharmacol 2023. [Epub ahead of print]. doi: 10.1111/bph.16232.
5. Hwang I, Kim JW, Ylaya K, et al. Tumor-associated macrophage, angiogenesis and lymphangiogenesis markers predict prognosis of non-small cell lung cancer patients. J Transl Med 2020;18:443.
6. Tan HW, Xu YM, Qin SH, et al. Epigenetic regulation of angiogenesis in lung cancer. J Cell Physiol 2021;236:3194-206.
7. Zhao C, Zhang J, Ma L, et al. GOLPH3 Promotes Angiogenesis of Lung Adenocarcinoma by Regulating the Wnt/β-Catenin Signaling Pathway. Onco Targets Ther 2020;13:6265-77.

8. Li X, Li H, Li Z, et al. TRPV3 promotes the angiogenesis through HIF-1α-VEGF signaling pathway in A549 cells. Acta Histochem 2022;124:151955.
9. Lu H, Wu C, Jiang XW, et al. ZLDI-8 suppresses angiogenesis and vasculogenic mimicry in drug-resistant NSCLC in vitro and in vivo. Lung Cancer 2023;182:107279.
10. Zhang J, Zeng Q, She M. The roles of FHL2 in cancer. Clin Exp Med 2023;23:3113-24.
11. Wang C, Lv X, He C, et al. Four and a Half LIM Domains 2 (FHL2) Contribute to the Epithelial Ovarian Cancer Carcinogenesis. Int J Mol Sci 2020;21:7751.
12. Gao X, Yang L. HBXIP knockdown inhibits FHL2 to promote cycle arrest and suppress cervical cancer cell proliferation, invasion and migration. Oncol Lett 2023;25:186.
13. Gao A, Su Z, Shang Z, et al. TAB182 aggravates progression of esophageal squamous cell carcinoma by enhancing β-catenin nuclear translocation through FHL2 dependent manner. Cell Death Dis 2022;13:900. Erratum in: Cell Death Dis 2023;14:270.
14. Li N, Xu L, Zhang J, et al. High level of FHL2 exacerbates the outcome of non-small cell lung cancer (NSCLC) patients and the malignant phenotype in NSCLC cells. Int J Exp Pathol 2022;103:90-101.
15. Pan B, Wan L, Li Y, et al. Comprehensive pan-cancer analysis identifies FHL2 associated with poor prognosis in lung adenocarcinoma. Transl Cancer Res 2023;12:1516-34.
16. Ma C, Tang X, Tang Q, et al. Curcumol repressed cell proliferation and angiogenesis via SP1/mir-125b-5p/VEGFA axis in non-small cell lung cancer. Front Pharmacol 2022;13:1044115.
17. Ahmed Z, Bicknell R. Angiogenic signalling pathways. Methods Mol Biol 2009;467:3-24.
18. Jiang T, Zhuang J, Duan H, et al. CD146 is a coreceptor for VEGFR-2 in tumor angiogenesis. Blood 2012;120:2330-9.
19. Qi Y, Song Y, Cai M, et al. Vascular endothelial growth factor A is a potential prognostic biomarker and correlates with immune cell infiltration in hepatocellular carcinoma. J Cell Mol Med 2023;27:538-52.
20. Eguchi R, Kawabe JI, Wakabayashi I. VEGF-Independent Angiogenic Factors: Beyond VEGF/VEGFR2 Signaling. J Vasc Res 2022;59:78-89.
21. Santoni G, Amantini C, Nabissi M, et al. Functional In Vitro Assessment of VEGFA/NOTCH2 Signaling Pathway and pRB Proteasomal Degradation and the Clinical Relevance of Mucolipin TRPML2 Overexpression in Glioblastoma Patients. Int J Mol Sci 2022;23:688.
22. Husain A, Khadka A, Ehrlicher A, et al. Substrate stiffening promotes VEGF-A functions via the PI3K/Akt/mTOR pathway. Biochem Biophys Res Commun 2022;586:27-33.
23. Hao M, Ding C, Sun S, et al. Chitosan/Sodium Alginate/Velvet Antler Blood Peptides Hydrogel Promotes Diabetic Wound Healing via Regulating Angiogenesis, Inflammatory Response and Skin Flora. J Inflamm Res 2022;15:4921-38.
24. Zhao ZT, Wang J, Fang L, et al. Dual-responsive nanoparticles loading bevacizumab and gefitinib for molecular targeted therapy against non-small cell lung cancer. Acta Pharmacol Sin 2023;44:244-54.
25. Cao Y, Liu YL, Lu XY, et al. Integrative analysis from multi-center studies identifies a weighted gene co-expression network analysis-based Tregs signature in ovarian cancer. Environ Toxicol 2024;39:736-50.
26. Amann T, Egle Y, Bosserhoff AK, et al. FHL2 suppresses growth and differentiation of the colon cancer cell line HT-29. Oncol Rep 2010;23:1669-74.
27. Jin X, Jiao X, Jiao J, et al. Increased expression of FHL2 promotes tumorigenesis in cervical cancer and is correlated with poor prognosis. Gene 2018;669:99-106.
28. Yao X, Zeng Y. Tumour associated endothelial cells: origin, characteristics and role in metastasis and anti-angiogenic resistance. Front Physiol 2023;14:1199225.
29. Hida K, Maishi N, Takeda R, et al. The Roles of Tumor Endothelial Cells in Cancer Metastasis. In: Sergi CM, editor. Metastasis. Brisbane (AU): Exon Publications; May 3, 2022.
30. Maiborodin I, Mansurova A, Chernyavskiy A, et al. Cancer Angiogenesis and Opportunity of Influence on Tumor by Changing Vascularization. J Pers Med 2022;12:327.
31. Zhu Y, Liu X, Wang Y, et al. DMDRMR promotes angiogenesis via antagonizing DAB2IP in clear cell renal cell carcinoma. Cell Death Dis 2022;13:456.
32. Wang Y, Han D, Pan L, et al. The positive feedback between lncRNA TNK2-AS1 and STAT3 enhances angiogenesis in non-small cell lung cancer. Biochem Biophys Res Commun 2018;507:185-92.
33. Schuster C, Akslen LA, Straume O. β2-adrenergic receptor expression in patients receiving bevacizumab

therapy for metastatic melanoma. Cancer Med 2023;12:17891-900.
34. Zhang H, Zhou J, Li J, et al. N6-Methyladenosine Promotes Translation of VEGFA to Accelerate Angiogenesis in Lung Cancer. Cancer Res 2023;83:2208-25.

Cite this article as: Chen T, Chen J, Chen Q, Liang Z, Pan L, Zhao J, She X. Promotion of non-small cell lung cancer tumor growth by *FHL2* via inducing angiogenesis and vascular permeability. J Thorac Dis 2024;16(2):1424-1437. doi: 10.21037/jtd-23-1975